Journal of the Brazilian Society of Mechanical Sciences and Engineering (2024) 46:602
https://doi.org/10.1007/s40430-024-05183-4

TECHNICAL PAPER

Structural analysis and sealing capacity of gasketed plate heat exchangers with HNBR and EPDM rubbers

Mateus de Sousa Zanzi[1] · Gabriel Benedet Dutra[2] · Giovani Silveira Magalhães Martins[1] · Guilherme Mariz de Oliveira Barra[1] · Jorge Luiz Goes Oliveira[2] · Kleber Vieira Paiva[2]

Received: 10 January 2024 / Accepted: 30 August 2024

Abstract
Rubber is an engineering polymer of interest in most industrial sectors. In gasketed plate heat exchangers (GPHEs), these elements comprise gaskets that are responsible for sealing the system under high levels of compression, temperature and pressure. Therefore, it is a necessity to understand how operating conditions affect GPHE structural behavior and sealing performance, regarding rubber materials and features. This work aims at determining GPHE integrity and mechanical characteristics with the aid of sealing performance experiments and strain gauge measurements at critical plate locations in a real equipment and in prototypes consisting of GPHE components. Hydrogenated nitrile butadiene rubber (HNBR) and ethylene-propylene-diene rubber (EPDM) gasket materials were evaluated. Based on compression strength experiments, the system stiffness ranged from approximately 0.3 to 7.0 kN/mm regarding the combined effects of the number of plates and the compression level. The combined effects of compressive strength, compression levels and rubber material on sealing performance were obtained with prototypes comprising at least six gaskets, whose conditions presented stable compressive strength behavior. In critical region on the real-scale heat exchanger, the measured von Mises stress level was 316 MPa and 133 MPa using EPDM and HNBR gaskets during tightening, respectively. It is conjectured that higher operation pressure loads can occur with the harder and stiffer material (EPDM), as showed by hydrostatic tests. Empirical correlations were developed in order to relate sealing capacity based on the system geometry, compression level and gasket material.

Keywords Gasketed plate heat exchanger · Sealing · Compression · EPDM · HNBR

1 Introduction

Ubiquitous industries (*e.g.,* chemical, petrochemical, the food and pharmaceutical sectors) use various types of heat exchangers (HE) to assure thermal control of their production lines [1, 2]. Among the available models, the gasketed plate heat exchanger (GPHE) is frequently chosen owing to its compactness and flexibility concerning design possibilities. The GPHE structure consists of plates (through which the heat exchange is carried out), gaskets, thick compression end-plates and bolts for tightening. The sealing mechanism of these systems guarantees the sealing of processing fluids under extreme environments. While subsea oil and gas production uses metal-to-metal sealing mechanism due to extreme environmental conditions [3], elastomeric gaskets provide sealing in GPHE systems [1].

Despite the use of metallic plate materials such as stainless steel and titanium which allow high temperature operations, gasket materials used in GPHE determine maximum working temperatures in these systems. Gaskets can be affected by environments containing oxygen, which roots rubber oxidation [2, 4, 5], and allow operating temperatures up to 200 °C for some specific gasket materials. According to Adolfsson [5], breakdown time along GPHE useful life is nearly 30%, whereas 68% of failures are related to gasket expulsion or the lack of gasket sealing capacity due to degradation of their properties, which highlights the importance of these components [6, 7]. Recent studies about GPHEs address heat exchanger failure modes and progress in these structures [5, 8], like corrosion

Technical Editor: João Marciano Laredo dos Reis.

✉ Mateus de Sousa Zanzi
mateus_zanzi@hotmail.com

[1] Department of Mechanical Engineering, Federal University of Santa Catarina, Florianópolis, SC 88040-900, Brazil

[2] Department of Mobility Engineering, Federal University of Santa Catarina, Joinville, SC 89218-035, Brazil

Published online: 11 September 2024

in stainless-steel plates [9, 10], fatigue [11, 12]. Other studies with GPHE focus on thermal and hydraulic performance under operation conditions, as well as the effects of plates geometry and operation parameters [13, 14]. Rubber materials studies have been recently studied in order to predict the O-rings and gaskets lifetime [15, 16] based on accelerated thermo-oxidative aging [17–20].

Common gasket materials used in oil and gas industries are nitrile butadiene rubber (NBR), hydrogenated nitrile butadiene rubber (HNBR), ethylene-propylene-diene rubber (EPDM), fluoroelastomer (FKM) e perfluoroelastomer (FFKM) [21]. NBR and HNBR materials are characterized by elevated chemical resistance, allowing applications in hazardous environments [22, 23]. EPDM rubbers are not used in applications involving oil; however, they support higher temperatures than other typical gaskets [24, 25]. FKM are commonly studied for use in extreme environments, like high temperatures [26].

The sealing capacity of these rubbers is seldom investigated in heat exchangers applications. Some recent researches address the sealing performance for hydrogen industry [27], including focusing on the composition of rubbers [28]. Applications for deep sea and high temperature for nitrile rubber also have been studied [29, 30]. Kömmling et al. monitored the variation of HNBR and EPDM properties for 1.5 years and related gasket failures with intense material property changes [16]. Liu and Lian investigated rubber failures for sealing mandrel hanger. They identified the reduction in rubber elasticity by monitoring internal stresses for weights above 150 ton [31]. Zheng and Li studied the behavior of HNBR rubbers by means of stress relaxation tests and finite element analysis [32]. Zuo et al. compared the sealing performance based on contact stress for HNBR sealing components by employing theoretical model and the finite element model considering the stress relaxation effect are established [33]. Hu et al. studied the sealing capacity packaging element and shown the existent relationship between axial load due to packing compression and the maximum difference pressure [34].

This work assesses the sealing behavior of HNBR and EPDM gaskets applied in GPHEs. Compression strength experiments with the aid of a prototype reproduce the GPHE assembling procedure. GPHE integrity and mechanical characteristics were evaluated with stain gauge measurements in HE plates and sealing experiments. The effects of tightening distance and sealing pressure on gasket performance were determined.

2 Experimental procedure

2.1 Materials

Experiments were executed with gasket plate heat exchangers consisting of HNBR and EPDM sealing materials, and stainless steel plates (SAE 316L). The corrugated wavy pattern plate shape is an outcome of cold forming. Martins et al. characterized the applied 316 plates using tensile tests on standardized tensile specimens extracted from the plate region where the gasket is present according to ASTM Standard Test Methods [35, 36]. Young's modulus (E) and Poisson's ratio (ν) were determined as 128 ± 12 GPa, and 0.31, respectively [35].

Gasket performance evaluation occurred with strain gauge measurements in different plate locations during GPHE assembly and with sealing tests, and with compression strength experiments in prototypes formed by gasket and plate segments. In the former, entire gaskets accommodated in the original plates were assessed with varying tightening distances and sealing pressures (Fig. 1a). In the latter, continuous circular gasket segments extracted from the branches of the GPHE inlet/outlet were coupled to corresponding plate segments (Fig. 1b).

Gasket material properties are defined as follows. Nitrile-based material (HNBR) comprises 96% hydrogenation, 36% acrylonitrile (C≡N), and an iodine value of 11 phr, while the EPDM rubber consists of 55 phr ethylene and 2.3 phr ethylidene norbornene (ENB). Gasket heights of both materials were determined as 4.113 ± 0.110 mm with a digital micrometer from Mitutoyo DSC250-X. Hardness values of 78.1 ± 0.6 and 81.5 ± 0.5 Shore A for HNBR and EPDM rubbers, respectively, were obtained with Mitutoyo HH 336 Shore A durometer with a standard measuring support (Mitutoyo 811–013), following ISO 7619–1 standards [37]. The gaskets have a complex cross-sectional geometry with nominal height of 4 mm and nominal width of 9 mm [15]. The prototype has an internal diameter of 110 mm which corresponds to 14% of the total length of a full-scale joint for this GPHE model.

2.2 Assembly

The assembly process of plate heat exchangers follows progressive compression stages so that gaskets reach the operating compression level determined by the design tightening distance. Table 1 presents typical compression levels obtained during the GPHE assembling procedure with the actual model of gasket and plates. The level 1.00A represents the ideal tightening distance (maximum tightness) specified by the manufacturer.

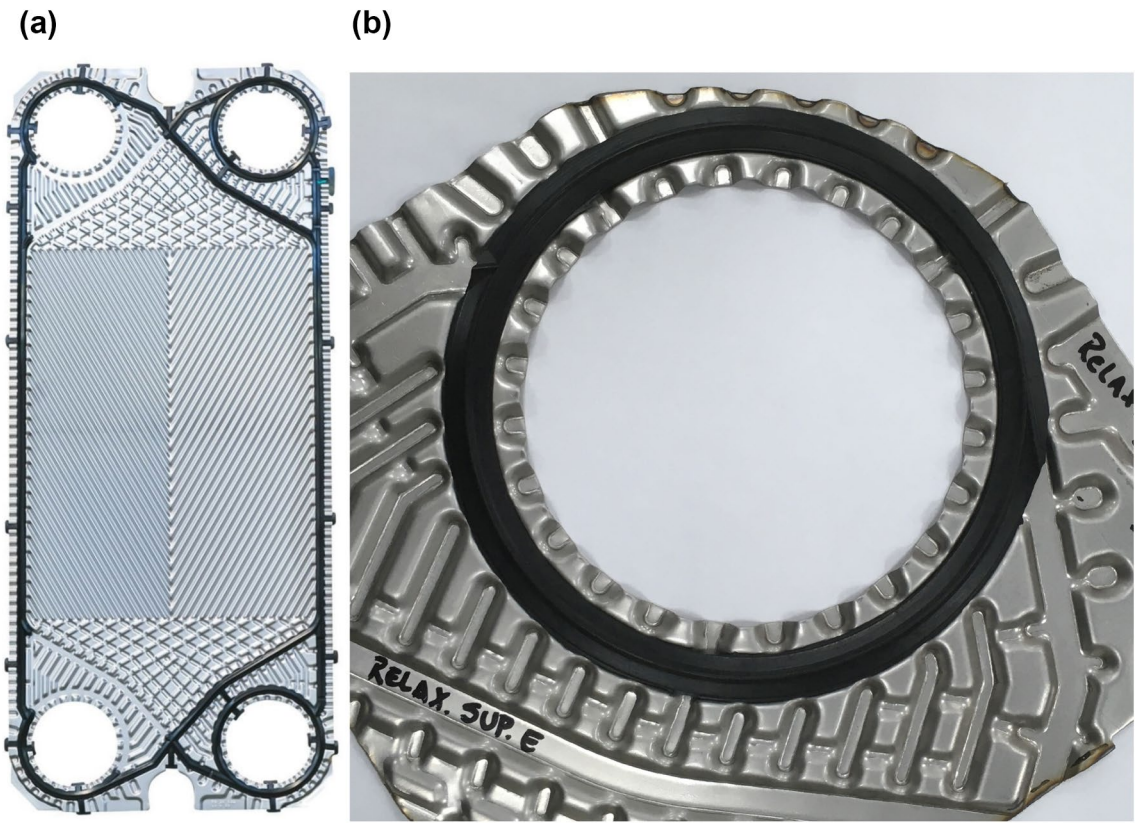

Fig. 1 Photographs of **a** GPHE plate and gasket and **b** gasket and plate segments

Table 1 Typical compression levels obtained during the GPHE assembling procedure

Tightening distance (A)	Gasket height (mm)	Compression level (%)
1.30	3.38	15.50
1.20	3.12	22.00
1.10	2.86	28.50
1.05	2.73	31.75
1.00	2.60	35.00

The assembly procedure follows Martins et al. [35]. Once a tightening distance is applied over the heat exchanger, periods of ten minutes allow gasket stress relaxation. The succeeding reduction in gasket stresses reduces the necessary work to reach the operating compression levels. Once the assembly is concluded and before the sealing tests are initiated, a thirty-minute interval provides the final relaxation.

2.3 Compression strength

The prototype was subjected to compression stress relaxation experiments by means of Instron 23–100 universal testing machine equipped with a 100 kN load cell (Instron CCE 100kN). The compression strength generated during the assembly was monitored. Porthole segments extracted from real-scale gaskets characterize the prototype specimens (Fig. 1). The continuous porthole gasket segment was selected since it consists of a closed boundary element and it can fit in the space designated for compression loads. Therefore, this element can better mimic the behavior of the closed real-scale gasket (Fig. 2).

The test temperature was set to 30 °C and controlled by a thermal chamber with an accuracy of ± 1 °C. Changes on the tightening distance (in accordance to Table 1) occurred with a displacement rate of 1 mm.min^{-1}. Following ISO 3384, the measured strength in relaxation experiments consists of values recorded 30 min after the desired compression plateau is reached [39]. Therefore, the measured stress after relaxation is the compression strength regarding the complex geometry of the prototype. Sets containing 1–16 gaskets provide the effect of the number of gaskets on the compression strength. With the above procedure, it is possible to identify the number of gaskets which provide a representative condition for GPHEs' behavior.

2.3.1 Stress analysis

Deformation measurements at specific plate locations were obtained with electrical resistance triaxial strain gauges

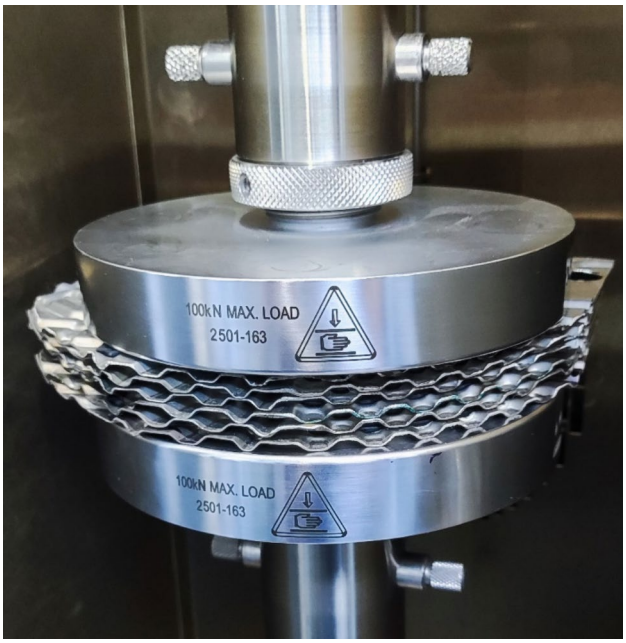

Fig. 2 Photograph of the prototype arrangement subjected to compression loads

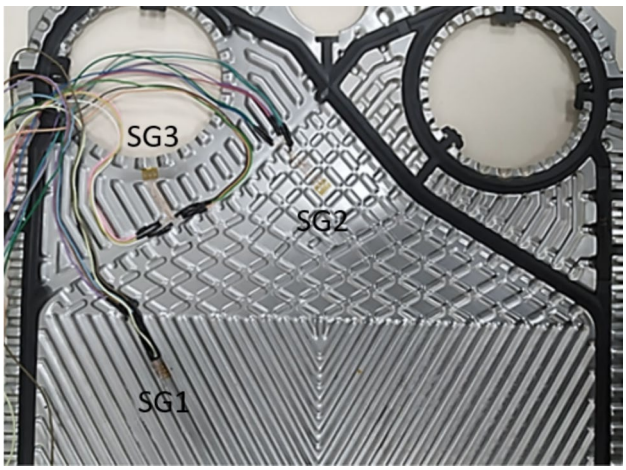

Fig. 3 Positioning of triaxial strain gauges at the heat exchange region (SG1), the fluid distribution area (SG2) and the gasket groove of the porthole region (SG3)

during GPHE assembly. Stress is then calculated in the elastic regime as applied by Martins et al. [25]. Strain gauge positioning followed the works of Martins et al. and Nascimento who presented GPHE main failure mechanisms [38, 40]. The strain gauges (SG) were positioned at the heat exchange region (SG1), the fluid distribution area (SG2) and the gasket groove of the porthole region (SG3), as shown in Fig. 3. Monitoring of plate deformations occurred in assembly experiments with EPDM and HNBR gaskets.

In the elastic region, stresses (σ) increase with increasing strain (ε) according to Hooke's Law. Due to the plate complex geometry, the principal strain directions are unknown. By considering isotropic material, the principal stresses ($\sigma_{p,q}$) are calculated as:

$$\sigma_{p,q} = \frac{E}{2}\left[\frac{\varepsilon_0 + \varepsilon_{90}}{1-\nu} \pm \frac{\sqrt{2}}{1+\nu}\sqrt{(\varepsilon_0 - \varepsilon_{45})^2 + (\varepsilon_{45} - \varepsilon_{90})^2}\right] \tag{1}$$

where the subscripts 0, 45 and 90 stands for strain directions. Multiaxial von Mises criterion determines von Mises equivalent stress (σ_{VM}) as:

$$\sigma_{VM} = \sqrt{\frac{\sigma_p^2 + \sigma_q^2 + \left(\sigma_p + \sigma_q\right)^2}{2}} \tag{2}$$

2.3.2 Equivalent stiffness

The unidirectional load applied in the prototype acts in the normal direction to the plate surface as illustrated in Fig. 2. Therefore, estimation of the gasket stiffness in the load direction is a simplification for obtaining the gasket compressive strength response and GPHE's stiffness, see Kelly e Konstantinidis [41].

The vertical stiffness of the elastomeric structure (K_g) consists of combining N gaskets in series. The stiffness determination is given by, Van Engelen [42]:

$$K_g = \frac{E_c A_{cs}}{y_0} \tag{3}$$

where A_{cs} is the vertical cross-sectional area, y_0 is the gasket height and E_c is the rubber compression modulus. The latter is a parameter related to the rubber shear modulus (G) and the shape factor (S):

$$E_c = 4GS^2 \tag{4}$$

For rubbers without holes, E_c is equal to $6GS^2$. However, considering ratios between inner and outer diameters greater than 0.5, the hole influence is significant and modifies E_c values to $4GS^2$, see reference [41]. The rubber shape factor (S) for annular geometry considers the ratio between the loaded area (cross-sectional area) and the free-surface area:

$$S = \frac{\left(d_o - d_i\right)}{2t} \tag{5}$$

where t is the rubber thickness, and d_i and d_o are the inner and outer diameters, respectively. By employing Eq. (4), different shear moduli result from different compression levels and number of gaskets. Note that E_c is related to rubber shear modulus and shape factor; however, it does not represent

gaskets properties but the combination of rubbers and plates in series, see reference [43].

The equivalent compression modulus (E_{eq}) can be calculated as a function of rubber compression and cross-sectional area (A_{cs}) [41]:

$$E_{eq} = \frac{P}{A_{cs}\varepsilon_y} \tag{6}$$

where P is the instant applied load and ε_y is the instant rubber vertical strain, obtained by:

$$\varepsilon_y = \frac{y_0 - y}{y_0} \tag{7}$$

where y is the instant height. By recording the load P 30 min after reaching each compression level mitigates viscous dissipation effects during rubber stress relaxation.

Despite the approach simplicity, it allows sealing capacity relationship between prototype and real-scale heat exchanger. Evaluation of heat exchanger sealing capacity is costly and time-consuming.

2.4 Sealing tests

A critical condition in experiments with GPHEs considers only one pressurized branch (*i.e.*, single-test condition), while another is free for deformation, which promotes elevated mechanical stresses [35, 38]. Regarding the pressurization systems, GPHE tests occurred with Flutrol equipment consisting of a hydro-pneumatic pump type Haskel ASF-35 (Fig. 4a), while pressurization of the prototype occurred with a Flutrol TestPac 33, consisting of a Haskel MS-71 hydro-pneumatic pump (Fig. 4b). The prototype comprises a pack of 6 gaskets. Hydrostatic experiments were performed only after fulfilling the sealing structures with water in ambient temperature (T ~ 23 °C), ensuring the air removal. An acquisition system and a pressure transducer (Omega PX409 750 psig) monitored the instant pressure from the inlet branch, controlled by a manual valve.

The pressure increment was adjusted to two bars. Three-minute interval was sufficient to detect leakage in both systems before reaching the next pressure steps, which characterizes an overall pressurization rate of 0.66 bar.min^{-1}. Static pressure reduction of 10% or more characterized a leakage event [15]. The pressure increase occurred for the same compression level. Experiments occurred with different tightening distances, ranging from 1.30 to 1A.

Experiments with GPHEs comprise a twenty-plate pack with the same gasket material. GPHEs can operate without leaks within a wide range of tightening distances stipulated by the manufacturer. The minimum tightening distance represents the leak-tight distance. However, during the operation of GPHEs, there are chances of leak events between minimum and maximum distances due to gasket aging or gasket displacement [15, 19].

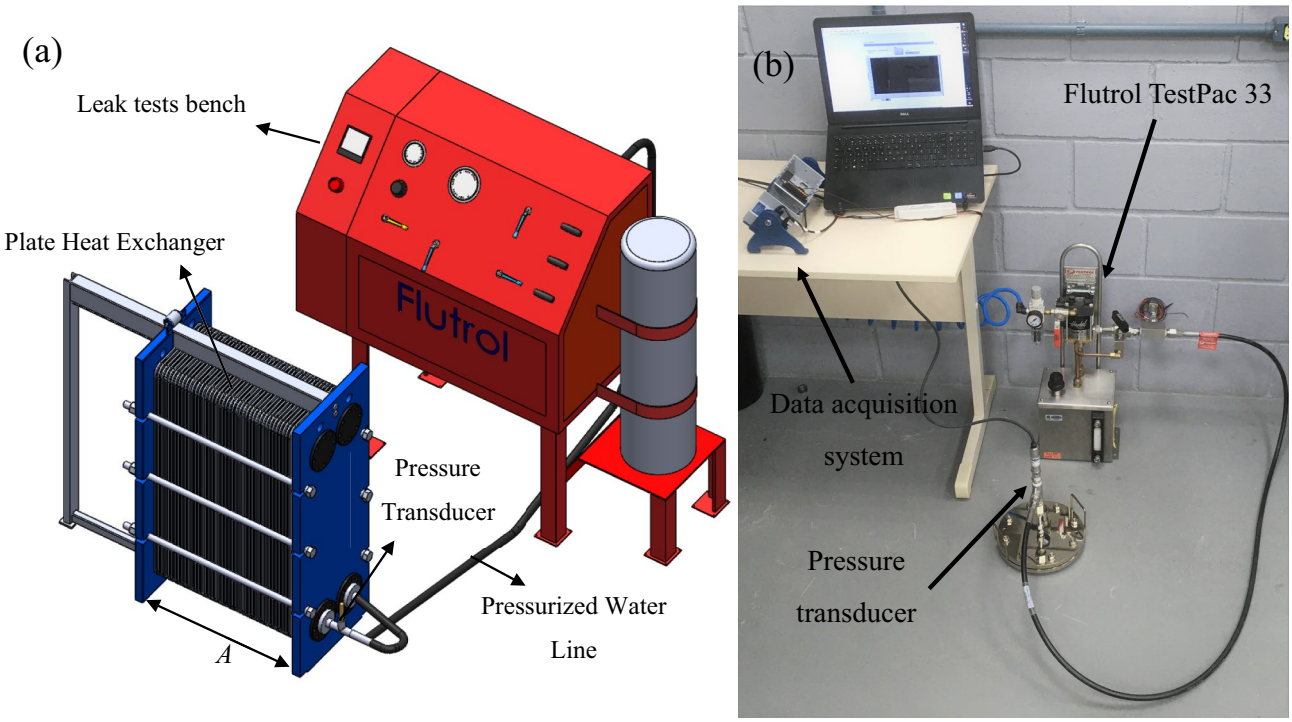

Fig. 4 Pressurization test benches for **a** GPHE [38] and **b** prototype [15]

3 Results and discussion

In this section, all experiments were evaluated with the aid of analysis of variance (ANOVA) within a confidence interval of 95%. Each experimental point is an average of five repetitions. Maximum standard deviation regarding the whole set of experiments is 5.1%.

3.1 Compression strength

Figure 5 presents the results of compression strength owing to stress relaxation experiments as function of the number of plates (*N*) with different tightening distances.

Compression strength increases with decreasing tightening distance, since the rubber strain also increases. The compression strength also increases by increasing the number of gaskets (*N*), when *N* ranges from 1 to 6. However, for prototypes consisting of 6 gaskets or more, a rigid body behavior stabilizes the pack's compression strength due to stiffness reduction [44, 45], as observed in Fig. 6. The compression strength is also affected by the interaction between the elastic (plate) and viscoelastic (rubber) components. HNBR compression strength reaches nearly 14 kN with experiments consisting of 6 gaskets or more, while EPDM gaskets reach about 30 kN.

Figure 6 shows the effects of compression strain and number of gaskets on the heat exchanger stiffness for EPDM and HNBR gaskets.

The GPHE stiffness increases with increasing compression strain and decreasing number of gaskets. EPDM gaskets show superior compression resistance and stiffness values as compared to those obtained with HNBR gaskets. This outcome is also related to superior hardness values for EPDM material as informed in Sect. 2.1, which results in a superior restriction to the mobility of rubber chains [46, 47].

Figure 7 shows the effect of compression strain on compression strength (P) for EPDM and HNBR gaskets (left y-axis). The dashed line stands for P_{EPDM}/P_{HNBR} strength ratio (right y-axis). Images at the top qualitatively represent

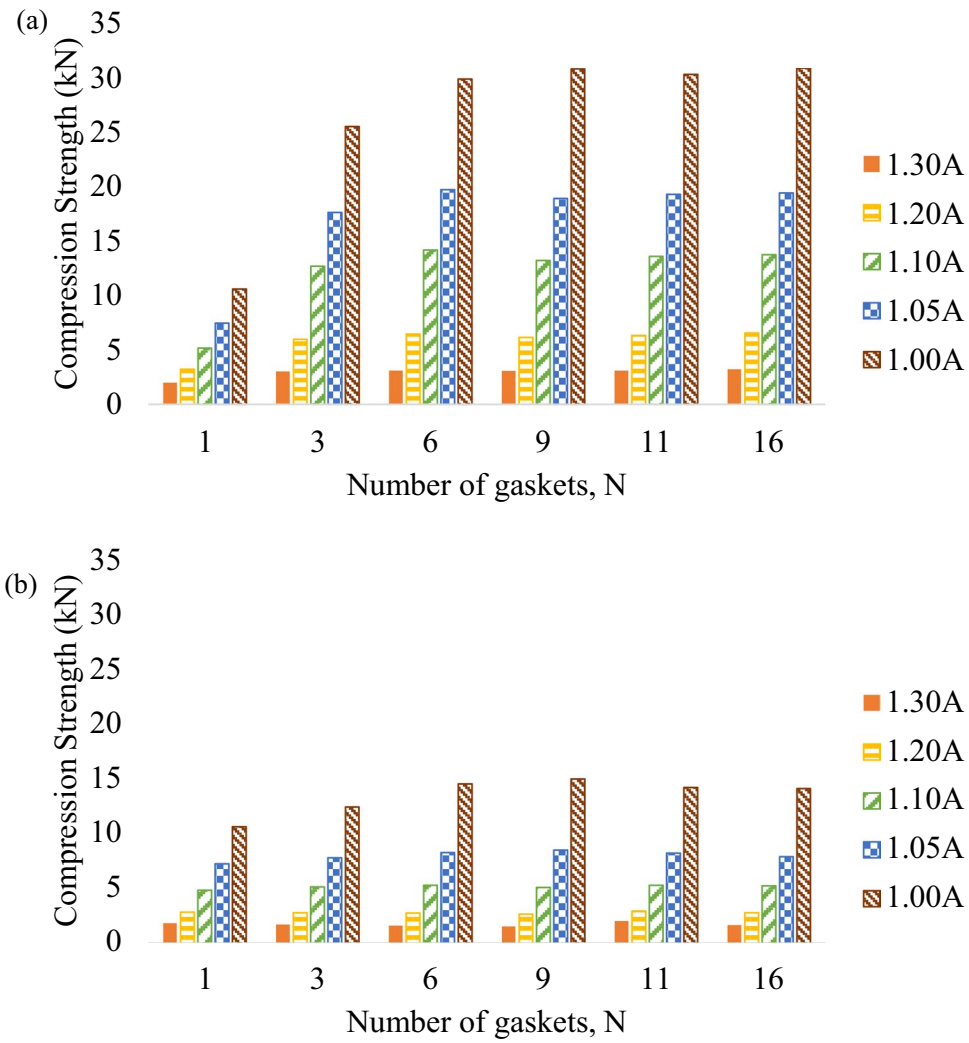

Fig. 5 Effects of tightening distance and number of gaskets on the HE compression strength: **a** EPDM and **b** HNBR gaskets

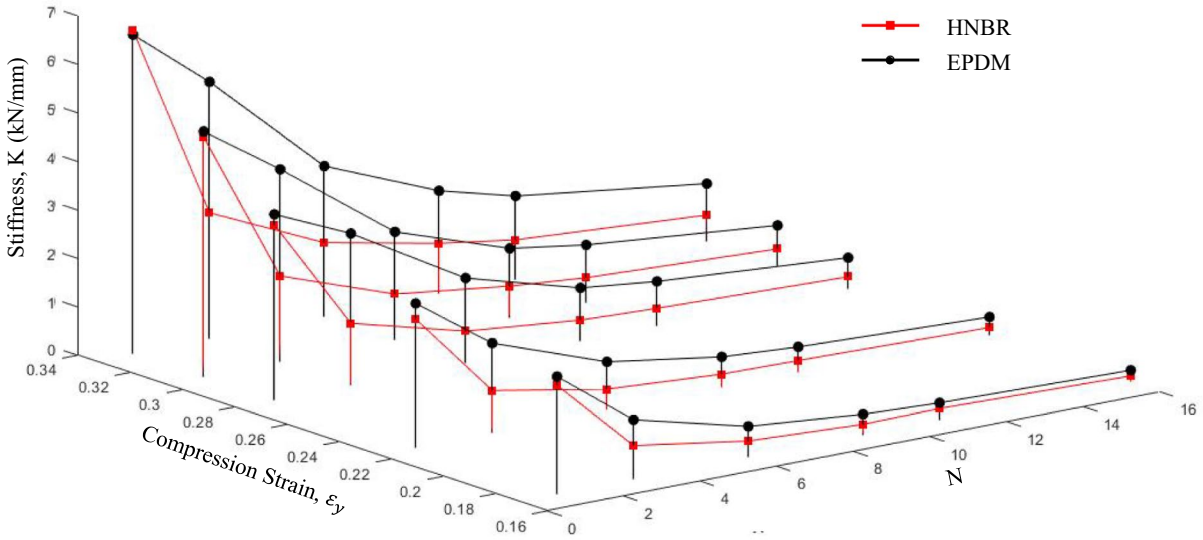

Fig. 6 Combined effects of compression strain and number of gaskets on the HE stiffness for EPDM and HNBR gaskets

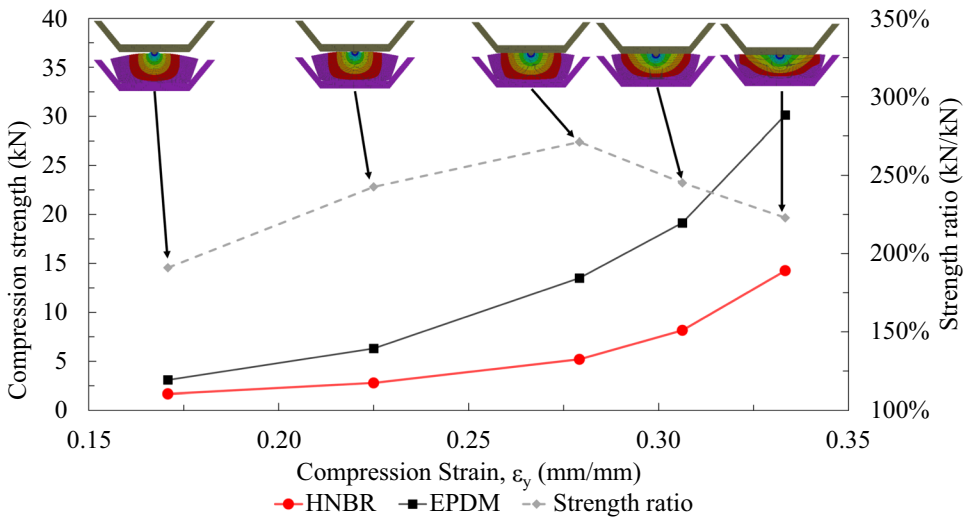

Fig. 7 Effect of compression strain on compression strength (*P*) for EPDM and HNBR gaskets (left *y*-axis). The dashed line stands for P_{EPDM}/P_{HNBR} strength ratio (right *y*-axis)

the decreasing tightening distance (regarding tightening steps) from left to right and the adaptation of the rubber in the groove.

Compression strength increases with increasing compression strain (see black and red lines) and decreasing tightening distances (see images at the top). Since the physical restriction imposed by the plates to gaskets' deformation increases with decreasing tightening distance, the compression strength increase tends to be exponential. When the tightening distance ranges from 1.3 to 1.1A (or compression strain ranges from 0.17 to 0.27), the gasket material has elevated influence on compression resistance, *i.e.*, the compression modulus approaches the properties of the material (rubber) since the aspect ratio is relatively low [42]. When the tightening distance ranges from 1.1 to 1.0A (or compression strain ranges from 0.27 to 0.33), the rubber influence on the final compression resistance decreases, *i.e.*, the gasket influence on the compression modulus (E_c) depends on the material, the restriction to deformation, and the thickness reduction, which affect the shape factor. Note that the strength ratio, P_{EPDM}/P_{HNBR} (right y-axis), decreases for compression strain over 0.27: gasket properties become less important.

In summary, the rubber compression strength during the tightening procedure is an outcome of the combined effects of the stiffness variation due to the number of gaskets,

tightening distance, gasket material properties, and restricted deformation.

3.2 GPHE assembling

Table 2 summarizes the stress levels obtained for five tightening distances in three different plate locations: heat exchange area, flow distribution area and nozzle, for EPDM and HNBR gaskets. Stress levels remained constant during the relaxation periods, as shown by references [35, 38]. When the tightening distance is 1A, the gasket height is equivalent to 2.6 mm.

The nozzle region has staggered gaskets to allow the inlet and outlet of working fluids. These gasket segments exert significant contact pressure on the plate to ensure sealing capacity, increasing stress levels. Consequently, the gasket type and material significantly influence the generated stress. Highest stress levels were obtained with EPDM gaskets due to elevated values of hardness, stiffness and compression strength. In the nozzle region and with the tightening distance equal to 1A, plate stress level was equal to 316 MPa for EPDM gasket and to 133 MPa for HNBR material. Superior stress levels for EPDM application on GPHE (2.38 times higher than HNBR application) agree with compression strength values previously presented (2.14 times higher for EPDM material as compared to HNBR one).

Figure 8 shows the effect of the tightening distance on GPHE von Mises stresses (left y-axis) and on the prototype compression strength (right y-axis). The results of GPHE stress levels are presented at the most requested region (nozzle area). The compression strength results are shown for prototypes with six gaskets.

Von Mises stresses and compression strength increase with decreasing tightening distance. Note that the compressive strength provided by EPDM gaskets yields substantial stresses as compared to HNBR gaskets.

Table 2 Effects of tightening distance and plate local area on Von Mises stress levels during heat exchanger assembly for EPDM and HNBR gaskets

Tightness (A)	Von Mises stress (MPa)					
	Exchange area		Distribution area		Nozzle	
	EPDM	HNBR	EDPM	HNBR	EPDM	HNBR
1.30	11.45	5.93	10.07	4.11	20.60	14.31
1.20	10.73	13.17	17.47	9.89	30.80	26.83
1.10	6.30	5.03	15.41	11.04	102.60	37.56
1.05	18.10	9.26	18.70	8.90	186.21	86.32
1.00	20.53	10.85	14.56	12.52	316.19	133.11

Note that the heat exchange and flow distribution areas are hardly affected by the GPHE assembling procedure, which indicates a slight interaction/contact between plates. However, in the nozzle region, the equivalent Von Mises stresses increase with decreasing tightening distance, as reported previously by Martins et al. [35, 38]

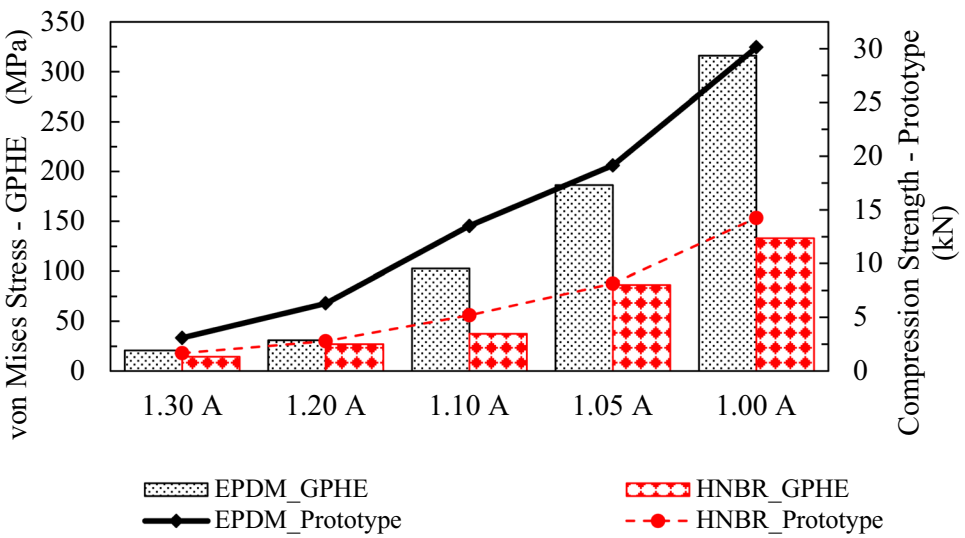

Fig. 8 Effect of the tightening distance on GPHE von Mises stresses (left *y*-axis) and on the prototype compression strength (right *y*-axis)

3.3 Sealing tests

Figure 9 shows the effect of compression strain on prototype and GPHE sealing capacity (or maximum supported pressure before leakage occurrence) for EPDM and HNBR gaskets. Black lines are related to EPDM results, and red lines, to HNBR results. The results are shown for prototypes with six gaskets and GPHE with 20 gaskets.

Leakage occurs in the interface between the plate and the gasket. The sealing capacity increases with increasing compression strain. High compression strains result in high contact stresses and compression strength, yielding superior sealing capacities and supported pressures. With the same compression strain, higher working pressures can be attained with EPDM gaskets owing to higher compression strengths as compared to HNBR gaskets. Furthermore, with the same compression strain, supported pressures in prototypes are more significant than the ones obtained with GPHEs. The structure that embraces the prototype is compacter and stiffer than the GPHE structure. Note that the prototype comprises a uniform and continuous geometry (circular) with greater robustness, while the GPHE has complex contact stress distribution along the gasket. The GPHE frame has been designed for working pressures up to 20 bar, and, therefore, it was not possible to identify the sealing capacity of GPHE experiments with EPDM gaskets when the compression strain was equal to 37% (corresponding to the tightening distance of 1A).

Table 3 shows empirical correlations obtained by linear regressions for sealing capacities (or maximum working pressures) of HNBR and EPDM gaskets, regarding experiments with prototypes and heat exchangers. The variables P, G and C denote prototype maximum pressure, GPHE maximum pressure and compression strain, in that order. The subscripts "E" and "H" stand for EPDM and HNBR gaskets, respectively. Equations that relate EPDM/HNBR and prototype/GPHE results are also provided. The quality of the correlations is expressed by R^2-values over 0.94. From these relationships, it is possible to estimate the maximum operating pressure of the heat exchanger based on tests performed on prototypes considering the gasket material used.

4 Conclusions

This study investigates the structural performance and sealing capacity of gasketed plate heat exchangers (GPHE) equipped with hydrogenated nitrile butadiene rubber (HNBR) and Ethylene Propylene Diene Monomer (EPDM) gaskets. Appraisal occurs with sealing and compression

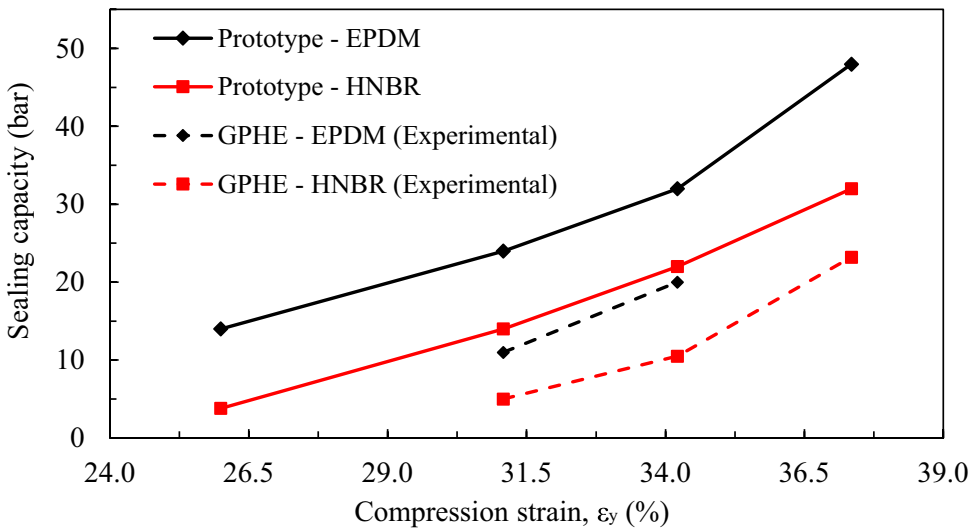

Fig. 9 Effect of compression strain on prototype and GPHE sealing capacity (or maximum work pressure) for EPDM and HNBR gaskets

Table 3 Sealing capacities (or maximum work pressures) for HNBR and EPDM gaskets

	Prototype	GPHE	Prototype/GPHE relationship
EPDM	$P_E = 2.88C - 63.21$	$G_E = 2.87C - 78.31$*	$P_E - G_E = 0.01C + 15.10$ *
HNBR	$P_H = 2.46C - 61.08$	$G_H = 2.91C - 86.55$	$P_H - G_H = -0.45C + 25.46$
EPDM/HNBR relationship	$P_E - P_H = 0.43C - 2.13$	$G_E - G_H = -0.04C + 8.24$	–

*From 1.10 to 1.05 A

strength experiments, and strain gauge measurements in heat exchangers and prototypes representing these structures.

The rubber compressive strength during the tightening procedure is an outcome of the combined effects of the stiffness variation due to the number of gaskets, tightening distance, gasket material properties, and restricted deformation. Compression strength increases with increasing compression strain and increasing number of gaskets. However, experiments in prototypes revealed stable strength levels for tests with six plates or more.

Regarding the employed gasket materials, prototypes with EPDM gaskets showed 30 kN in the last tightening step (1A) of the compressive strength tests compared to 14 kN with HNBR ones. This outcome is also related to superior hardness values for EPDM material, which results in a superior restriction to the mobility of rubber chains. The resulting stiffness values ranged from 0.3 to 7.0 kN/mm.

Comparing to heat exchangers experiments, the prototype compression strength is directly related to the elevated stress levels measured at specific plate areas during tightening procedure. During tightening procedure with the real-scale heat exchanger, the resulting von Mises stress level in critical region was 316 MPa and 133 MPa using EPDM and HNBR gaskets, respectively. Since von Mises stresses increases with decreasing tightening distance, we conclude that the heat exchanger stiffness increases with compression strain and decreases with number of gaskets.

The sealing capacity of the evaluated systems increases with increasing compression strain, as well as compressive strength and supported working pressures. Therefore, with the same compression strain level, higher working pressures can be attained with EPDM gaskets owing to higher compressive strengths as compared to HNBR gaskets. Finally, empirical correlations were obtained to relate sealing capacity and compression level for EPDM and HNBR gaskets. These correlations allow the relationship of the sealing capacity between prototype and real-scale heat exchanger, since the sealing capacity assessment of the heat exchanger is costly and time-consuming.

Acknowledgements We would like to express our gratitude to FAPESC, CAPES, CNPq, PETROBRAS S.A, and Agência Nacional de Petróoleo, Gás Natural e Biocombustível (ANP) for supporting this research.

Declarations

Conflict of interest The authors declare that they have no known competing financial interests or personal relationships that could have appeared to influence the work reported in this article.

References

1. Shah RK, Sekulić DP (2003) Fundamentals of heat exchanger design. John Wiley & Sons, Hoboken
2. Kakaç S, Liu H, Pramuanjaroenkij A (2020) Heat exchangers: selection, rating, and thermal design, 4th edn. CRC Press, Boca Raton
3. Li Y, Zhao H, Wang D, Xu Y (2020) Metal sealing mechanism and experimental study of the subsea wellhead connector. J Braz Soc Mech Sci Eng 42:26. https://doi.org/10.1007/s40430-019-2112-1
4. Wang L, Sundén B, Manglik RM (2007) Plate heat exchangers: design, applications and performance. WIT Press, Southampton, Boston
5. Arsenyeva O, Tovazhnyanskyy L, Kapustenko P et al (2023) Review of developments in plate heat exchanger heat transfer enhancement for single-phase applications in process industries. Energies 16:4976. https://doi.org/10.3390/en16134976
6. Adolfsson R (2016) Life cycle assessment and life cycle cost of heat exchangers: a case for inter terminals Sweden AB located in Port of Gothenburg. Master's thesis, Chalmers University of Technology
7. Rydén L (2003) Field reliability of plate heat exchangers in oil and gás process—A market perspective. M. Sc. Dissertation, Lund University
8. Ali M, Ul-Hamid A, Alhems LM, Saeed A (2020) Review of common failures in heat exchangers—Part I: mechanical and elevated temperature failures. Eng Fail Anal 109:104396. https://doi.org/10.1016/j.engfailanal.2020.104396
9. Fan ZD, Du JS, Zhang ZB et al (2019) Internal leakage of plate heat exchangers caused by cooperation of pitting, crevice corrosion, and fretting. Eng Fail Anal 96:340–347. https://doi.org/10.1016/j.engfailanal.2018.10.007
10. Gagliardi A, Lanzutti A, Simonato M et al (2018) Failure analysis of a plate heat exchanger used in a blast chiller. Eng Fail Anal 92:289–300. https://doi.org/10.1016/j.engfailanal.2018.06.005
11. Pelliccione AS, SantAnna R, Siqueira MHS et al (2019) Failure analysis of a titanium plate heat exchanger—Mechanical fatigue. Eng Fail Anal 105:1172–1188. https://doi.org/10.1016/j.engfailanal.2019.07.059
12. Hoseinzadeh S, Heyns PS (2020) Thermo-structural fatigue and lifetime analysis of a heat exchanger as a feedwater heater in power plant. Eng Fail Anal 113:104548. https://doi.org/10.1016/j.engfailanal.2020.104548
13. dos Santos FJ, Martins GSM, Strobel M et al (2024) Combined effects of inlet conditions and assembly accuracy on Nusselt and friction factors of plate heat exchangers. Int J Therm Sci 197:108797. https://doi.org/10.1016/j.ijthermalsci.2023.108797
14. Strobel M, Beckedorff LE, Martins GSM et al (2024) Experiments on gasketed plate heat exchangers with segmented corrugation pattern. ASME J Heat Mass Transf 10(1115/1):4065453
15. Zanzi MS, de Souza EL, Dutra GB et al (2022) Service lifetime prediction of nitrile butadiene rubber gaskets used in plate heat exchangers. J of Appl Polym Sci. https://doi.org/10.1002/app.52523
16. Kömmling A, Jaunich M, Pourmand P et al (2019) Analysis of O-ring seal failure under static conditions and determination of end-of-lifetime criterion. Polymers 11:1251. https://doi.org/10.3390/polym11081251
17. De Ruijter PQ, De Bittencourt RE, Zanzi MDS et al (2024) HNBR and NBR gasket rubbers for plate heat exchangers: thermo-oxidative aging and service lifetime prediction. J Appl Polym Sci 141:e55055. https://doi.org/10.1002/app.55055
18. de Souza EL, de Sousa ZM, de Paiva KV et al (2022) Thermo-oxidative aging of acrylonitrile-butadiene rubber gaskets with real

geometry used in plate heat exchangers. J Appl Polym Sci. https://doi.org/10.1002/app.53419
19. Kömmling A, Jaunich M, Pourmand P et al (2017) Influence of ageing on sealability of elastomeric O-rings. Macromol Symp 373:1600157. https://doi.org/10.1002/masy.201600157
20. Qiu D, Liang P, Peng L et al (2020) Material behavior of rubber sealing for proton exchange membrane fuel cells. Int J Hydrogen Energy 45:5465–5473. https://doi.org/10.1016/j.ijhydene.2019.07.232
21. Patel H, Salehi S, Ahmed R, Teodoriu C (2019) Review of elastomer seal assemblies in oil & gas wells: performance evaluation, failure mechanisms, and gaps in industry standards. J Petrol Sci Eng 179:1046–1062. https://doi.org/10.1016/j.petrol.2019.05.019
22. Lou W, Zhang W, Liu X et al (2017) Degradation of hydrogenated nitrile rubber (HNBR) O-rings exposed to simulated servo system conditions. Polym Degrad Stab 144:464–472. https://doi.org/10.1016/j.polymdegradstab.2017.09.009
23. Lainé E, Grandidier JC, Benoit G et al (2019) Effects of sorption and desorption of CO2 on the thermomechanical experimental behavior of HNBR and FKM O-rings—Influence of nanofiller-reinforced rubber. Polym Testing 75:298–311. https://doi.org/10.1016/j.polymertesting.2019.02.010
24. Cui T, Chao YJ, Van Zee JW (2012) Stress relaxation behavior of EPDM seals in polymer electrolyte membrane fuel cell environment. Int J Hydrogen Energy 37:13478–13483. https://doi.org/10.1016/j.ijhydene.2012.06.098
25. Pourmand P, Hedenqvist MS, Furó I, Gedde UW (2017) Deterioration of highly filled EPDM rubber by thermal ageing in air: kinetics and non-destructive monitoring. Polym Testing 64:267–276. https://doi.org/10.1016/j.polymertesting.2017.10.019
26. Jin L, Xue Z, Wang Z et al (2023) Mechanical response of the sealing packer based on two rubber materials at high temperatures. Polym Testing 124:108073. https://doi.org/10.1016/j.polymertesting.2023.108073
27. Zhou C, Zheng Y, Hua Z et al (2024) Recent insights into hydrogen-induced blister fracture of rubber sealing materials: an in-depth examination. Polym Degrad Stab 224:110747. https://doi.org/10.1016/j.polymdegradstab.2024.110747
28. Clute C, Balasooriya W, Cano Murillo N et al (2024) Morphological investigations on silica and carbon-black filled acrylonitrile butadiene rubber for sealings used in high-pressure H2 applications. Int J Hydrogen Energy 67:540–552. https://doi.org/10.1016/j.ijhydene.2024.04.133
29. Wu J-B, Li L, Wang P-J (2024) Effect of stress relaxation on the sealing performance of O-rings in deep-sea hydraulic systems: a numerical investigation. Eng Sci Technol, Int J 51:101654. https://doi.org/10.1016/j.jestch.2024.101654
30. Zhang J, Li Q, Zhang C et al (2024) High-temperature sealing performance and structure optimization of rubber core for conical blowout preventer. Geoenergy Sci Eng 234:212606. https://doi.org/10.1016/j.geoen.2023.212606
31. Liu Y, Lian Z (2021) Failure analysis on rubber sealing structure of mandrel hanger and improvement in extreme environments. Eng Fail Anal 125:105433. https://doi.org/10.1016/j.engfailanal.2021.105433
32. Zheng X, Li B (2021) Study on sealing performance of packer rubber based on stress relaxation experiment. Eng Fail Anal 129:105692. https://doi.org/10.1016/j.engfailanal.2021.105692
33. Zuo R, Wang G, Hu G et al (2022) Theoretical research on sealing performance of packing element used in the dual gradient packer considering stress relaxation effect. J Braz Soc Mech Sci Eng 44:237. https://doi.org/10.1007/s40430-022-03530-x
34. Hu G, Wang G, Li M et al (2018) Study on sealing capacity of packing element in compression packer. J Braz Soc Mech Sci Eng 40:438. https://doi.org/10.1007/s40430-018-1364-5
35. Martins GSM, Zanzi MS, De Paiva KV et al (2023) Mechanical stress analysis of various GPHE corrugated plates during the assembly and in working conditions. Int J Press Vessels Pip 206:105013. https://doi.org/10.1016/j.ijpvp.2023.105013
36. E28 Committee (2013) ASTM E8 Standard Test Methods for Tension Testing of Metallic Materials
37. (2010) ISO 7619–1—Rubber, vulcanized or thermoplastic: determination of indentation hardness—Part 1: durometer method (Shore hardness). ISO—International Organization for Standardization, Switzerland
38. Martins GSM, Santiago RS, Beckedorff LE et al (2022) Structural analysis of gasketed plate heat exchangers. Int J Press Vessels Pip 197:104634. https://doi.org/10.1016/j.ijpvp.2022.104634
39. (2005) ISO 3384—Rubber, vulcanized or thermoplastic: determination of stress relaxation in compression at ambient and elevated temperatures. ISO—International Organization for Standardization, Switzerland
40. Nascimento (2013) Structural Behavior Analysis of Plate Heat Exchangers. Master Thesis, Federal University of Rio de Janeiro
41. Kelly JM, Konstantinidis DA (2011) Mechanics of rubber bearings for seismic and vibration isolation, 1st edn. Wiley, Hoboken
42. Van Engelen NC (2019) Fiber-reinforced elastomeric isolators: a review. Soil Dyn Earthq Eng 125:105621. https://doi.org/10.1016/j.soildyn.2019.03.035
43. Van Engelen NC, Tait MJ, Konstantinidis D (2016) Development of design code oriented formulas for elastomeric bearings including bulk compressibility and reinforcement extensibility. J Eng Mech 142:04016024. https://doi.org/10.1061/(ASCE)EM.1943-7889.0001015
44. Rao SS (2011) Mechanical vibrations, 5th edn. Prentice Hall, Upper Saddle River
45. Inman DJ (2014) Engineering vibration, 4th edn. Pearson, Boston
46. De SK, White JR (2001) Rubber technologist's handbook. Rapra Technology, Shrewsbury
47. Canevarolo SV (2020) 9—Polymer mechanical behavior. In: Canevarolo SV (ed) Polymer science. Hanser, Munich, pp 237–279